Organic–inorganic semiconductor devices and 3, 4, 9, 10 perylenetetracarboxylic dianhydride: an early history of organic electronics

2003 J. Phys.: Condens. Matter 15 S2599

(http://iopscience.iop.org/0953-8984/15/38/001)

INSTITUTE OF PHYSICS PUBLISHING JOURNAL OF PHYSICS: CONDENSED MATTER

J. Phys.: Condens. Matter **15** (2003) S2599–S2610 PII: S0953-8984(03)64737-5

Organic–inorganic semiconductor devices and 3, 4, 9, 10 perylenetetracarboxylic dianhydride: an early history of organic electronics

S R Forrest

Center for Photonics and Optoelectronic Materials (POEM), Department of Electrical Engineering, Princeton University, Princeton, NJ 08544, USA

E-mail: forrest@ee.princeton.edu

Received 13 June 2003
Published 12 September 2003
Online at stacks.iop.org/JPhysCM/15/S2599

Abstract

The demonstration, over 20 years ago, of an organic–inorganic heterojunction (OI HJ) device along with investigations of the growth and physical properties of the archetypal crystalline molecular organic semiconductor 3, 4, 9, 10 perylenetetracarboxylic dianhydride are discussed. Possible applications of OI HJ devices are introduced and the dramatic change in conductive properties of these materials when exposed to high-energy ion beams is described. The past and future prospects for hybrid organic-on-inorganic semiconductor structures for use in electronic and photonic applications are also presented.

1. Organic-on-inorganic semiconductor devices

The first organic-on-inorganic semiconductor heterojunction (HJ) was demonstrated at Bell Laboratories in 1981, although the objective of these early investigations was not the demonstration of an electronic device [1]. Rather, they were directed at understanding the properties of the organic semiconductor 3, 4, 9, 10 perylenetetracarboxylic dianhydride (PTCDA), i.e. $C_{24}O_6H_8$. Only a few years earlier, the first conductive polymer, polyacetylene $-(CH)_n$ had been developed [2, 3]. Hence, by the early 1980s, investigations were underway in many laboratories to develop other, hopefully more stable conducting compounds. Martin Kaplan (a chemist) and Paul Schmidt (a metallurgist) had identified the compound PTCDA as a material that, when pyrolized, would change from a presumed closely stacked crystal into a linked polymer chain. Hence, they proceeded to expose the material to temperatures as high as 500 °C and found that this process resulted in a conductive, carbon-rich compound. To more fully understand the morphological and electronic transformation that PTCDA undergoes on pyrolization, we embarked on an investigation of its properties before and after the thermal process. The test structure that was used to investigate the as-deposited characteristics was the first organic–inorganic (OI) semiconductor diode, which consisted of a metal contact and

a 100–500 nm thick layer of PTCDA deposited onto the surface of a p-type Si substrate [1]. It was anticipated that the PTCDA in the untreated state was an insulator, and that the structure would result in a simple metal–insulator–Si (MIS) capacitor from which the dielectric constant and breakdown voltage of the organic could be inferred.

Surprisingly, rather than MIS capacitor characteristics, it was found that PTCDA formed a rectifying contact on Si, resulting in nearly ideal characteristics, analogous to those formed by a conventional p–n junction made in the same material as the substrate (figure 1). In particular, the forward-biased characteristics were influenced by the purity of the organic thin film, which was pre-cleaned using standard thermal gradient sublimation methods [4]. Under reverse bias, the junction leakage was primarily dominated by the generation and recombination of charges within the bulk of the Si substrate. Interestingly, both n- and p-type substrates, not only of Si but also of such materials as GaAs and InP, formed rectifying junctions when in contact with an organic semiconductor layer.

The observation that rectifying current–voltage characteristics of OI diodes were obtained on p- and n-type substrates of many different common group IV and III–V semiconductors raised several questions about the nature of the junction formed between the organic and inorganic semiconductors. Indeed, while PTCDA yielded nearly ideal rectifying characteristics following the Shockley equation, namely

$$J = J_s\{1 - \exp[-qV/nkT]\} \tag{1}$$

many other perylene- and naphthalene-based analogues to PTCDA were also found to perform at least qualitatively similarly to this model compound [5]. In (1), J is the current density, J_s is the saturation current density, q is the electronic charge, V is the voltage, kT is the thermal energy at temperature T, and n is the ideality factor. For PTCDA on Si, $1.5 < n < 2$, whereas for other organic materials and substrates the ideality factor was somewhat higher [5].

Early observations of the OI contact suggested that it could be modelled as a Schottky-like metal–semiconductor junction, but this picture did not explain the ability to rectify on both p- or n-type semiconductor substrates. Hence the 'Schottky' model was replaced by the picture of the OI contact as an HJ between an undoped (nearly intrinsic) organic semiconductor contacting a doped inorganic semiconductor substrate [6]. The rectifying junction is then formed by the energy offset between the frontier orbitals of the organic and the conduction or valence band minima of the inorganic semiconductor. Given that the organic materials contained a very small free-charge density, however, an additional aspect to this model was included. That is, unlike conventional semiconductor HJs, the Fermi energy of the organic was almost completely determined by the density of charge injected from the metal contact on its surface, or across the organic/inorganic HJ. The significant movement of the quasi-Fermi energy from its mid-energy gap position could also result in a change in the energy level offset at the OI HJ interface—possibly allowed to shift its position by an intervening oxide layer residing on the inorganic semiconductor surface [7, 8]. A proposed energy level diagram [6] of an OI HJ under reverse and forward bias, and at equilibrium, is shown in figure 2.

We note, however, that the equilibrium position of the Fermi energy, and hence the conductive properties of PTCDA [9], may also be affected by environmental exposure: there have been suggestions that, once exposed to air, the equilibrium Fermi level moves from near the lowest unoccupied toward the highest occupied molecular orbital (HOMO), thus suggesting atmospheric p-type doping [10]. All of these early experiments were performed in air.

With this picture, the current–voltage characteristics of PTCDA thin films, as well as many OI HJ rectifiers, could be modelled accurately and understood over their entire operating voltage and temperature range. It was also observed that charge transport across the PTCDA film was primarily by injected hole conduction, following Child's Law for a semiconductor

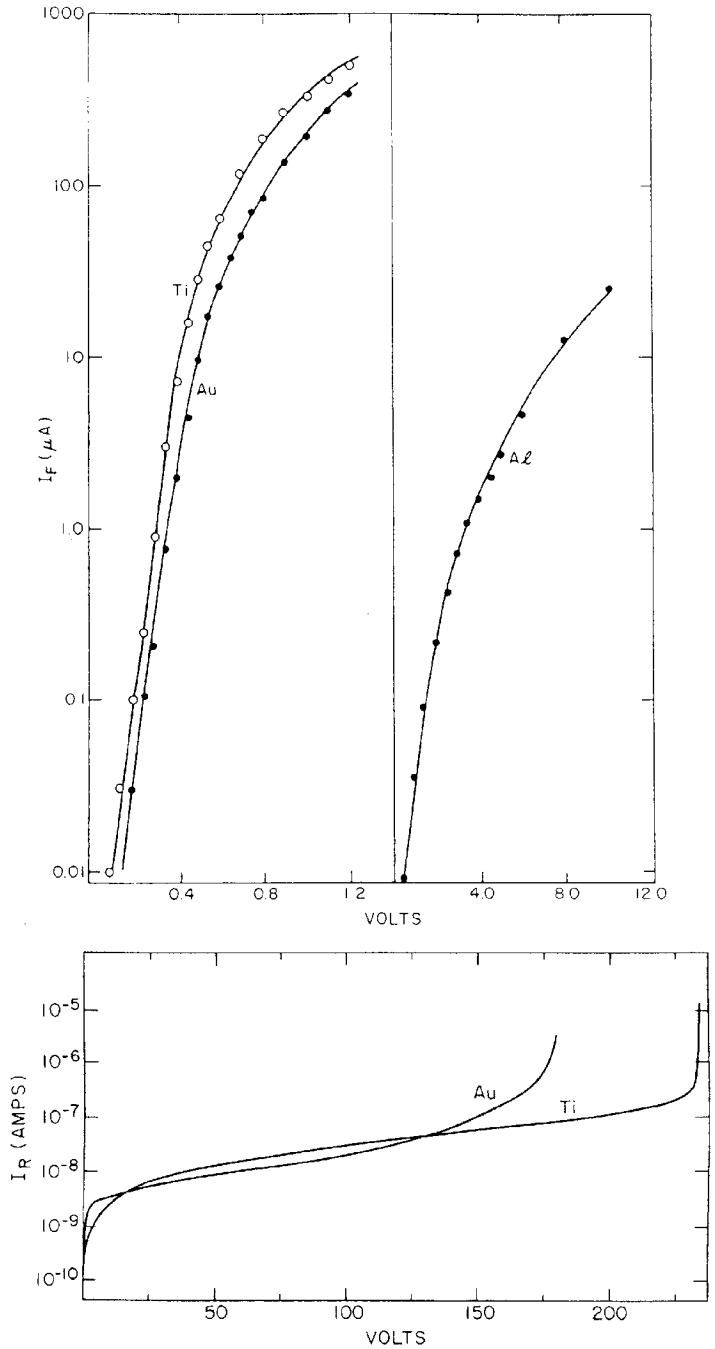

Figure 1. (a) The forward- and (b) reverse-biased current–voltage characteristics of a metal/100 nm PTCDA/10 Ω cm p-Si substrate for metal contact areas of 2.5×10^{-4} cm^2. The fits to the data are shown by the solid curves, and approximately follow equations (1) and (2) in the text. Note that Al forms a highly resistive (rectifying) contact to PTCDA, in contrast to Ti and Au, resulting in a higher forward voltage and ideality factor for the former device. Also, note that the reverse-biased characteristics are limited by generation–recombination current until, in the case of the Ti contact, avalanche breakdown in the Si substrate occurs [1].

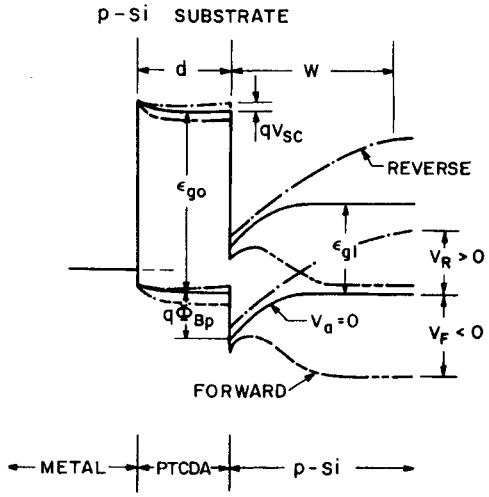

Figure 2. A proposed energy level diagram of a PTCDA/p-Si OI diode under equilibrium, and under forward and reverse bias [6].

with a moderate density of shallow traps [6], i.e.

$$J = \tfrac{9}{8}\varepsilon\mu_{\mathrm{p}}V^2/d^3 \tag{2}$$

where ε is the film permittivity, $\mu_{\mathrm{p}} = \mu_{\mathrm{p0}}p_{\mathrm{inj}}/P_{\mathrm{t}}$ is the mobility in the presence of trap density P_{t}, μ_{p0} is the mobility of the pristine (or trap-free) film, and d is the film thickness. Also, p_{inj} is the injected hole density, depending on the applied voltage. This space-charge limited transport (SCL) model was strongly supported by data such as that in figure 3, where we show the J–V characteristics of a PTCDA film that is sandwiched between an ohmic Ti contact and a rectifying Au contact [6]. At $V > 0.1$ V, the data clearly follow equation (2) over four decades in current. At lower voltages, the film transport is ohmic, from which we infer a free hole concentration of 5×10^{14} cm^{-3}.

2. Conductivity, order and thin film growth

While there remains some discussion today whether PTCDA is preferably a hole or electron conductor, this distinction has perhaps been a primary source of confusion in characterizing organic semiconductors in general. While the dianhydride groups of PTCDA are electron withdrawing, suggesting that it should behave as an n-type semiconductor, this is not the most important factor determining the conductive properties of the material. As in all crystalline solids, the relative *mobilities* of electrons and holes are determined by the crystal structure itself. That is, the extent of the overlap of the HOMO compared to that of the lowest unoccupied molecular orbital (LUMO) levels between neighbouring molecules determines whether the hole or electron mobility, respectively, is the larger.

In the case of PTCDA that was purified by multiple thermal gradient sublimation cycles, we have found consistently that hole mobility varies between $\mu_{\mathrm{p}} = 0.01$ and 1 cm^2 V^{-1} s^{-1} in thin films grown under ultra-high-vacuum growth conditions. As expected, higher mobilities are achieved under growth conditions that lead to a higher degree of stacking order [5] (see figure 4). The electron mobility (μ_{n}) in our materials prepared by this method have been unmeasurable, since it is considerably smaller than μ_{p}. There have been suggestions that the

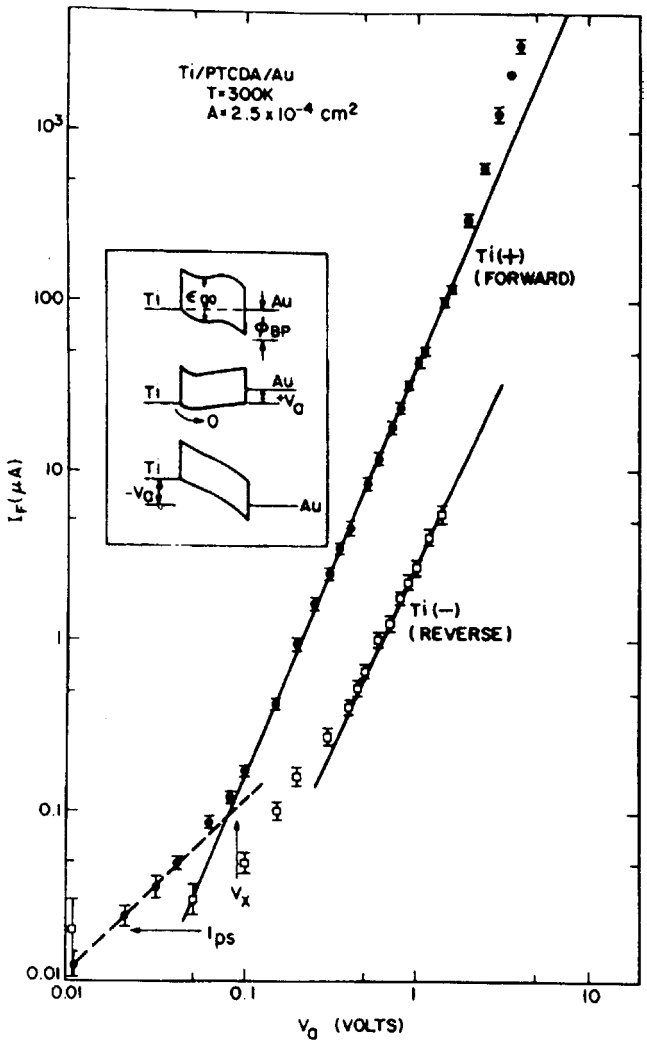

Figure 3. The forward- and reverse-biased characteristics for a Ti/200 nm PTCDA/Au 'Schottky' barrier diode, where the Au/PTCDA contact is rectifying. Two regions are apparent: at $V < V_x = 0.1$ V the current follows Ohm's Law and is carried by the background carriers in PTCDA ($\sim 5 \times 10^{14}$ cm^{-2}); at higher voltages the current scales as V^2, which is consistent with space-charge limited current (see equation (2)) [6].

discrepancy between reports by some groups [11] that $\mu_n > \mu_p$ lies in the large anisotropy that is inherent in the PTCDA crystal structure. For example, Ostrick *et al* [12] found that the hole mobility is larger than that of electrons along the stacking direction, whereas the opposite situation is found parallel to the stacks. Following the work on OI diodes and many subsequent investigations of the growth and electronic properties of PTCDA, this issue of carrier mobility still remains somewhat unresolved.

After the demonstration of high-performance OI HJ devices, further examination of PTCDA suggests that it is a truly remarkable electronic material, largely as a result of its crystal structure (see figure 5) [5]. The molecules form closely spaced, highly ordered planar π–π stacks, with an intermolecular packing distance along the stacks of just 3.21 Å, whereas

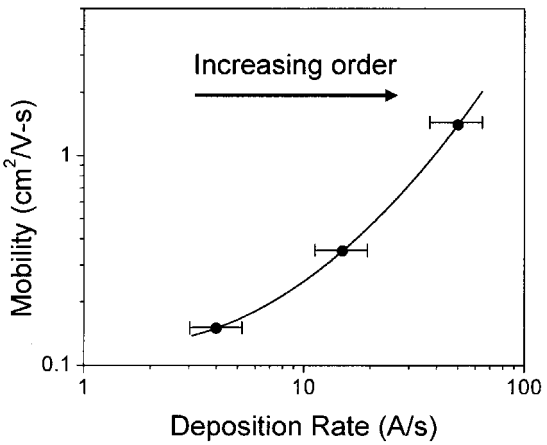

Figure 4. The hole mobility of 100 nm thick films of PTCDA deposited onto the surface of a 0.5 Ω cm p-Si substrate, inferred by fitting the forward-biased current–voltage characteristics to the expressions in (1) and (2). Using x-ray diffraction, it was found that increasing order is obtained at higher deposition rates, and that this corresponds to an increased hole mobility [5].

the spacing between stacks is significantly greater. This structural anisotropy, in turn, results in a very large anisotropy in the conductivity as well as a strong affinity to forming well ordered stacks and structures during growth. Indeed, PTCDA thin films behave as one-dimensional conductors, with current confined to directions that are parallel to the molecular stacking direction, which is typically normal to the substrate surface.

In addition to the exceptionally large anisotropy in conductivity, the structural anisotropy also results in thin film birefringence [13], with the index of refraction parallel to the plane equal to $n_{\parallel} = n_{\perp} + \Delta n$, compared to the out-of-plane index of $n_{\perp} = 1.36$, where $\Delta n = 0.66$. This giant birefringence has many potential implications in the application of PTCDA as an optical material.

The stacking habit of PTCDA is characterized by strong x-ray reflections from the planar stacking (102) planes [5]. More interesting, however, was the observation that PTCDA would self-organize spontaneously over large areas on amorphous substrates such as glass. The first observation of this self-organization is shown in figure 6, where two x-ray pole figures of the (102) Bragg reflection are shown for films grown at high and low growth rates (figures 6(a) and (b), respectively) [5]. The contours indicate regions of equal peak reflection intensity. At low growth rates, the peak intensity is approximately unchanged over all azimuthal directions, as is typical of a powder, suggesting that the growth is highly disordered. Surprisingly, at higher growth rates, the film becomes highly ordered. Indeed, although there is some dispersion in the exact position of the stacking direction of the (102) planes, there is a strong preference for stacking at $\pm 11^{\circ}$ to the substrate normal across the entire area covered by the $\sim(1\ \mathrm{mm})^2$ x-ray beam. From these data, we conclude that the film is highly—though not perfectly—ordered, as one would expect of a twinned crystal suggested by the texture map in figure 6(a). If this were a true twinned crystal, the contours would be far more tightly clustered along two spots at $\pm 11^{\circ}$. Nevertheless, this remarkable observation suggests that there is considerable crystalline alignment over large areas, even in the absence of an epitaxial templating of PTCDA with the glass substrate. This self-organization—with no commensurate relationship between the film structure and that of the substrate—was termed 'quasi-epitaxy' [14, 15].

This self-ordering is now understood to result from the strong interplanar van der Waals forces characteristic of such a tightly coupled system of molecular stacks. Its observation

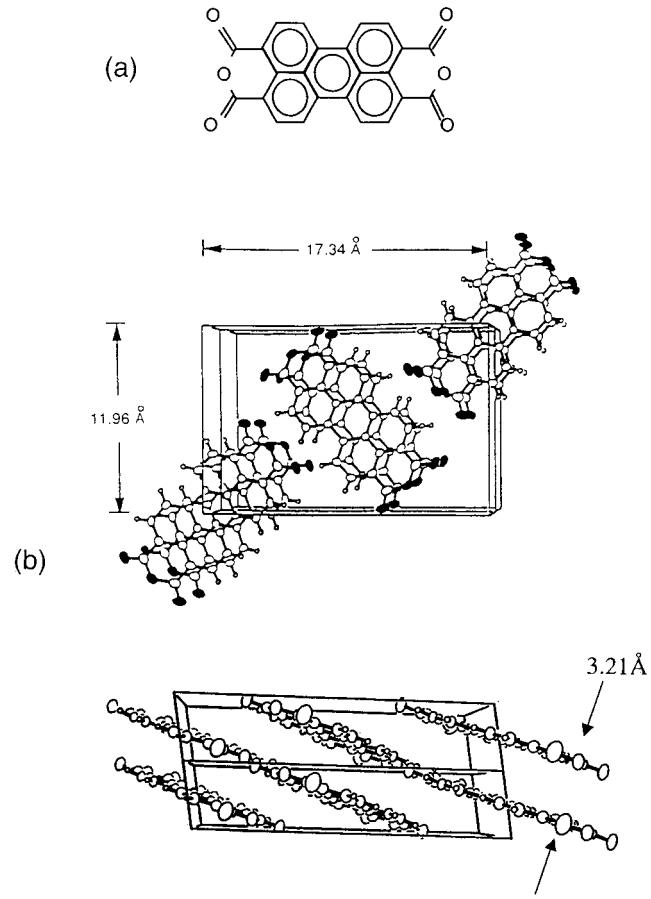

Figure 5. (a) The chemical structural formula of 3, 4, 9, 10 PTCDA. (b) The unit cell of PTCDA along two perpendicular projections. The unit cell is monoclinic, with the closest intermolecular separation along the (102) direction.

has led to considerable subsequent studies of molecular self-assembly of this and similarly fascinating π-stacking, planar molecular systems. In this regard, PTCDA has become the most commonly investigated organic crystalline material to be investigated for its growth properties using vacuum deposition and, in particular, the ultra-high-vacuum process of organic molecular beam deposition (OMBD), where the purity and control over the thin film structure can be controlled precisely [4, 14, 16]. Thus, PTCDA has been essential in developing our understanding of the nature of organic thin film growth and the range of structures that can be achieved by growth from the vapour phase.

3. Some applications of OI devices

While OI HJ devices are simple to fabricate and have remarkable—sometimes nearly ideal—electrical characteristics, and while PTCDA and its family of sister compounds such as 3, 4, 7, 8 napthalenetetracarboxylic dianhydride (NTCDA), have gained considerable attention from the scientific community for the last 20 years, it remains unclear as to what, if any, application niches these devices can fill. Nevertheless, immediately following the first

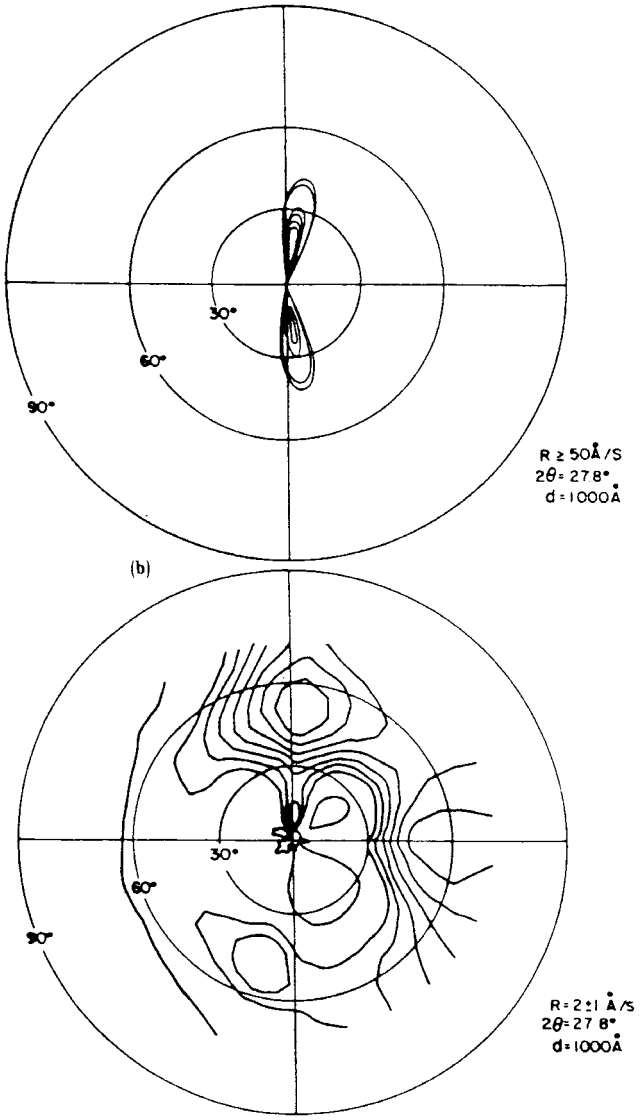

Figure 6. An x-ray pole figure for 100 nm thick PTCDA films grown on a glass substrate at growth rates of (a) 50 $Å^{-1}\ s^{-1}$ and (b) 2 $Å^{-1}\ s^{-1}$. For (a), the intensity decrease between each contour line (starting in the centre of each wing of the 'bow tie') is 10%, whereas in (b) the difference between contours is only 1%. These figures correspond to the intensity of the (102) Bragg reflection at all azimuthal angles shown [5].

demonstration of a rectifying OI HJ, these devices were used as a non-destructive probe for measuring the free-carrier density in the underlying semiconductor wafer [17, 18]. By reverse biasing the OI HJ, the free-charge density from the inorganic semiconductor surface to well within its bulk can be profiled using standard capacitance–voltage analysis. Then, by probing an array of metal contacts corresponding to an array of locations across a semiconductor wafer surface, free-carrier concentration 'maps' are generated [17], thereby providing an assessment of the properties and uniformity of the underlying semiconductor. Once these data are collected, the organic film with its contact array can be removed from the semiconductor surface using

a non-destructive, selective etchant, such as a lightly basic solution that does not attack the semiconductor itself.

The most successful early demonstration of this analysis technique was in the measurement of the conduction band offset energies (ΔE_c) of a series of InGaAsP/InP epitaxial wafers using PTCDA-based OI HJ contacts [18]. This material system is the foundation of modern long-haul fibre-optic communications devices, so an accurate knowledge of the HJ offset is critical to high-performance device design. By employing OI HJs on a series of wafers with different compositions of InGaAsP, we found that $\Delta E_c = 0.24\ \Delta E_g$, where ΔE_g is the difference in energy gap between a particular composition of InGaAsP and InP.

In a more recent application, the ability of the highly birefringent PTCDA to self-organize even on amorphous substrates was exploited in a waveguide-coupled detector. In this case, PTCDA served as a waveguide when deposited on a 10 μm wide polymer (Teflon^{TM}) ridge whose refractive index is less than either $n_\perp$ and $n_\parallel$. This ridge then served to input the long-wavelength ($\lambda = 1.064\ \mu$m) light into the edge of an integrated $In_{0.53}Ga_{0.47}As$ photodiode [19]. Due to the ordered deposition of the molecular stacks tilted parallel to the edges of the polymer ridge, the optical axis of the PTCDA film is aligned parallel to the ridge along the entire 2 cm length of the waveguide. This optical axis alignment allows for the preservation of the input polarization without any observed rotation along the entire waveguide length [19, 20]. Further, the absence of high-angle crystalline grain boundaries along the propagation direction minimizes light scattering, resulting in low optical loss. Such birefringence can be used in polarization-maintaining and polarization-selective devices. The high stability of PTCDA and its analogues is also promising for device applications where a long-term operational lifetime of the photonic devices is essential.

4. Conducting forms of PTCDA and its analogues

As noted in section 1, work on PTCDA and on OI HJ devices was motivated by the search for a stable conducting polymer. Early attempts at transforming the crystalline source material of PTCDA into a conductive material were directed at pyrolization of the material at high temperatures. However, Schmidt and co-workers [21] had early indications that local damage that was induced by electron beams drastically changed the optical properties of the material. It was thought that these local changes might be accompanied by changes in the conductivity as well. To test this assumption, large film areas were exposed to high-energy ion beams [22]. On impact with the organic films, the high-energy ions trigger a secondary-electron shower, which in turn can break numerous bonds of the as-deposited molecules. This leads to damage observed in lines just a few nanometres wide, produced by focused electron beams [21].

Indeed, it was found that the conductivity could be increased by 14 decades on exposure to 10^{17} cm^{-2} doses of 2 MeV Ar^+, as shown in figure 7(a). Maximum conductivities of 10^4 S cm^{-1}, or approximately that of the in-plane conductivity of graphite, were obtained consistently, not only in polyacenes such as PTCDA and NTCDA but also in the phthalocyanines and even in polymers. These local changes in conductivity were found to be limited by hopping between conductive islands separated by non-conducting barriers of varying widths. Such variable-range hopping is characterized by the following functional form in film resistivity [22]:

$$\rho = \rho_0 \exp\sqrt{T_0/T} \tag{3}$$

where T_0 is a characteristic temperature and ρ_0 is the resistivity at $T \to \infty$. From figure 7(b), it is apparent that equation (3) is followed over a very wide range of temperatures and ion doses. Further analysis then showed that the conducting islands were microcrystalline graphite domains [23].

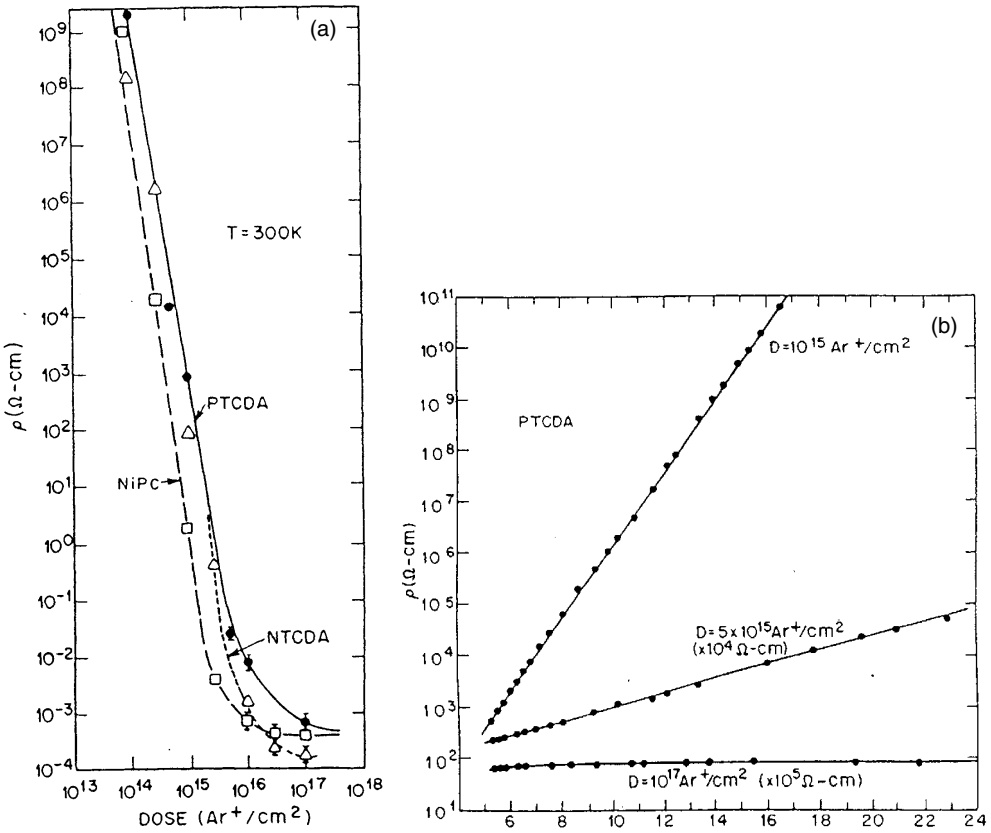

Figure 7. (a) The dependence of film resistivity on the dose of 2 MeV Ar^+ ions for three organic materials: PTCDA, NTCDA and Ni-phthalocyanine (NiPc). (b) The temperature dependence of the resistivity of a PTCDA thin film for three different dose levels. Note that, at the highest doses, the temperature dependence vanishes, which is characteristic of a disordered conducting solid. At lower dose levels, in the conductivity transition region the resistivity follows equation (3), which is consistent with conduction via variable-range hopping [22].

Thus, while the initial attempts at forming a conductive polymer—starting with the planar stacking compound PTCDA—were unsuccessful, the ability to increase the conductivity locally and dramatically by exposure to energetic particle beams provided an opportunity to 'write' conductors, even at the nanometre scale, in advanced electronic circuit applications. It should be noted that the morphological and chemical properties of the conductive regions are also altered considerably from those of the unexposed regions, allowing for the selective processing and fabrication of these two regions in a film where both the organic semiconductor and its converted conductive forms coexist on a single substrate.

5. The future of OI HJ devices and the ordered growth of organic thin films

Many OI HJ devices have been proposed and demonstrated—including their use in non-destructive semiconductor wafer bulk and surface defect analysis [7, 8, 24] —both as OI transistors with improved gate rectifying characteristics [25] and even as high-performance photodetectors [26]. In addition, these same materials lend themselves to significant structural

manipulation through growth and even through exposure to energetic particle beams, where highly conductive nanometre-wide regions can be produced. However, to date, no clear advantage for a simple OI HJ has been achieved over conventional or even all-organic devices. Hence, there is as yet no compelling case for their application in modern electronic systems.

Nevertheless, many new applications may be emerging where such hybrid devices will find uses. These possibly include nonlinear optical elements and even memory devices. While it remains to be seen which applications will emerge, the rapidly growing interest in organic electronics will almost certainly open a niche for OI HJ devices based on their very high performance and simplicity of fabrication.

Beyond applications, however, lies the wealth of knowledge in the physics of organic semiconductors that has been afforded by the work that has been undertaken worldwide since the early 1980s on the remarkable, archetypal compound PTCDA [4]. Controlled OMBD growth has led to unprecedented film quality, which has allowed exploration of the spectroscopic and conductive properties of this material in films with ordered structures and of thicknesses from a sub-monolayer all the way to several microns. Hence PTCDA, whose first electronic 'application' was in an OI HJ, has opened up a wide avenue for the understanding of organic materials in general. Analogues of PTCDA are showing particular promise for use in transistors [12, 27], organic solar cells [28] and photodetectors [29]. Thus, the lessons learnt and accumulated over the years about the physical and thin film properties of this remarkable organic semiconductor are certain to provide a further basis for the rapid advances in organic electronics that are currently being reported by laboratories around the globe.

Acknowledgments

The author is particularly indebted to Martin L Kaplan and Paul H Schmidt for their contributions to the understanding of OI HJs, ion-irradiated organic thin films, and a plethora of organic devices based on PTCDA and related compounds. He is also grateful to the US Air Force Office of Scientific Research, which supported much of his early work on OI HJs and subsequent work on advanced organic electronic devices.

References

[1] Forrest S R, Kaplan M L, Schmidt P H, Feldmann W L and Yanowski E 1982 *Appl. Phys. Lett.* **41** 90
[2] Chiang C K, Fincher C R Jr, Park Y W, Heeger A J, Shirakawa H and Louis E J 1977 *Phys. Rev. Lett.* **39** 1098
[3] Shirakawa H, Louis E J, McDiarmid A G, Chiang C K and Heeger A J 1977 *Chem. Commun.* 578
[4] Forrest S R 1997 *Chem. Rev.* **97** 1793
[5] Forrest S R, Kaplan M L and Schmidt P H 1984 *J. Appl. Phys.* **56** 543
[6] Forrest S R, Kaplan M L and Schmidt P H 1984 *J. Appl. Phys.* **55** 1492
[7] Forrest S R, Kaplan M L and Schmidt P H 1986 *J. Appl. Phys.* **60** 2406
[8] Forrest S R and Schmidt P H 1986 *J. Appl. Phys.* **59** 513
[9] Hirose Y, Aristov V, Soukiassian P, Bulovic V, Forrest S R and Kahn A 1996 *Phys. Rev.* B **54** 13748
[10] Kampen T U, Park S and Zahn D R T 2002 *J. Vac. Sci. Technol.* B **21** 879
[11] Karl N 1989 *Mol. Cryst. Liq. Cryst.* **171** 157
[12] Ostrick J R, Dodabalapur A, Torsi L, Lovinger A J, Kwock E W, Miller T M, Galvin M, Berggren M and Katz H E 1997 *J. Appl. Phys.* **81** 6804
[13] Zang D Y, So F F and Forrest S R 1991 *Appl. Phys. Lett.* **59** 823
[14] So F F, Forrest S R, Shi Y Q and Steier W H 1990 *Appl. Phys. Lett.* **56** 674
[15] Zhang Y and Forrest S R 1993 *Phys. Rev. Lett.* **71** 2765
[16] Forrest S R and Burrows P E 1997 *Supramol. Sci.* **4** 127
[17] Forrest S R, Kaplan M L, Schmidt P and Gates J V 1985 *J. Appl. Phys.* **57** 2982
[18] Forrest S R, Schmidt P H, Wilson R B and Kaplan M L 1984 *Appl. Phys. Lett.* **45** 1199
[19] Taylor R B, Burrows P E and Forrest S R 1997 *IEEE Photonics Technol. Lett.* **9** 365

[20] Zang D Y, Shi Y Q, So F F, Forrest S R and Steier W H 1991 *Appl. Phys. Lett.* **58** 562
[21] Schmidt P H, Joy D C, Kaplan M L and Feldmann W L 1982 *Appl. Phys. Lett.* **40** 93
[22] Forrest S R, Kaplan M L, Schmidt P H, Venkatesan T and Lovinger A J 1982 *Appl. Phys. Lett.* **41** 708
[23] Venkatesan T, Forrest S R, Kaplan M L, Murray C A, Schmidt P H and Wilkins B J 1983 *J. Appl. Phys.* **54** 3150
[24] Forrest S R, Kaplan M L and Schmidt P H 1987 *Annu. Rev. Mater. Sci.* vol 17, ed R A Huggins (Palo Alto, CA: Annual Reviews) p 192
[25] Cheng C-L, Forrest S R, Kaplan M L, Schmidt P H and Tell B 1985 *Appl. Phys. Lett.* **47** 1217
[26] So F F and Forrest S R 1989 *IEEE Trans. Electron. Devices* **36** 66
[27] Xue J and Forrest S R 2001 *Appl. Phys. Lett.* **79** 3714
[28] Tang C W 1986 *Appl. Phys. Lett.* **48** 183
[29] Peumans P, Yakimov A and Forrest S R 2003 *J. Appl. Phys.* **93** 3693